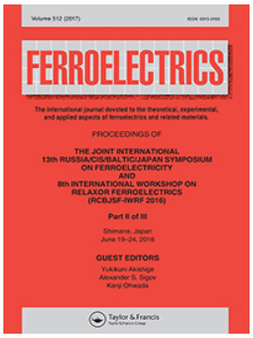


Ferroelectrics

ISSN: 0015-0193 (Print) 1563-5112 (Online) Journal homepage: https://www.tandfonline.com/loi/gfer20

# Raman scattering and phase transitions in fluorides with elpasolite structure

Alexander Vtyurin, Alexander Krylov, Vladimir Voronov & Svetlana Krylova

**To cite this article:** Alexander Vtyurin, Alexander Krylov, Vladimir Voronov & Svetlana Krylova (2017) Raman scattering and phase transitions in fluorides with elpasolite structure, Ferroelectrics, 512:1, 58-64, DOI: 10.1080/00150193.2017.1349863

**To link to this article:** https://doi.org/10.1080/00150193.2017.1349863

Published online: 09 Aug 2017.

FERROELECTRICS
2017, VOL. 512, 58–64
https://doi.org/10.1080/00150193.2017.1349863

Taylor & Francis
Taylor & Francis Group



# Raman scattering and phase transitions in fluorides with elpasolite structure

Alexander Vtyurin, Alexander Krylov, Vladimir Voronov, and Svetlana Krylova

Kirensky Institute of Physics SB RAS, Krasnoyarsk, Russia

**ABSTRACT**
Raman scattering spectra of $Rb_2KHoF_6$ and $Rb_2KDyF_6$ crystals have been studied in temperature range from 20 K to 399 K and from 7 K to 500 K respectively. Raman spectra of $Rb_2KHoF_6$ crystal are distorted due to the fluorescence process. Parameters of Raman lines have been quantitatively analyzed. The investigation points to the considerable role of $CX_6$ groups in the temperature phase transition in $Rb_2KHoF_6$ and $Rb_2KDyF_6$ crystals. The anomalies of spectra changes with temperature testify the first order phase transitions in these crystals.

**ARTICLE HISTORY**
Received 19 June 2016
Accepted 27 March 2017

## Introduction

The perovskite-like $Rb_2KHoF_6$ and $Rb_2KDyF_6$ crystals belong to the family of $A_2BCX_6$ elpasolites, where A, B, C are metal cations or more complex molecular ions and X are oxygen or halogen anions (high symmetry phase $G_0$, space group $Fm3m$, $Z = 4$). The crystalline, ceramic, and film materials with perovskite-like structures are widely used as functional elements due to their remarkable properties [1–8]. Temperature and pressure changes in fluorides cause a number of structural phase transitions, which are generally related to changes in the lattice of octahedral groups, such as small pivoting of $CX_6$ octahedra and displacement of Rb atoms. In particular, these changes manifest themselves experimentally in substantial anomalies in the crystal lattice dynamics, including the condensation of soft phonon modes during displacive transitions. The soft mode condensation has been successfully observed before in other elpasolites [9–14]. The structural properties and phase transitions of $Rb_2KHoF_6$ and $Rb_2KDyF_6$ crystals were studied by optical microscopy and calorimetry [15]. These crystals demonstrate phase transition under cooling at 403 K (into $G_1$ phase, space group $P12_1/n1$, $Z = 2$) for $Rb_2KHoF_6$ and 392 K (into $G_1$ phase, space group $P12_1/n1$, $Z = 2$) for $Rb_2KDyF_6$.

## Experiment

Raman scattering spectra of $Rb_2KHoF_6$ and $Rb_2KDyF_6$ crystals have been studied in temperature range from 20 K to 399 K and from 7 K to 500 K correspondingly. Because of the small sample size we could not observe polarized Raman spectra. Raman spectra were

**CONTACT** Alexander Vtyurin vtyurin@iph.krasn.ru Kirensky Institute of Physics SB RAS, Krasnoyarsk 660036, Russia.

collected in a backscattering geometry, using a triple monochromator Jobin Yvon T64000 Raman spectrometer operating in double subtractive mode then detected by a CCD cooled at 140 K. The spectral resolution for the recorded Stokes side Raman spectra was set to 1 $cm^{-1}$ (this resolution was achieved by using gratings with 1800 grooves $mm^{-1}$ and 100 $\mu$m slits). The microscope system based on Olympus BX41 microscope with a 50 × objective lens $f = 10.6$ mm of NA 0.5 provides a focal spot diameter of about 5 $\mu$m on a sample. Single-mode argon 514.5 nm of Spectra-Physics Stabilite 2017 $Ar^+$ laser of 100 mW power (15 mW on a sample) was used as excitation light source. We fitted the spectra using damped harmonic oscillator functions. Approximation of internal mode positions was performed using the dependence which corresponds to decay into two phonons:

$$\Omega(T) = \Omega_0 + A\left(1 + \frac{1}{\exp(c\hbar\Omega_{\beta 1} / k_B T) - 1} + \frac{1}{\exp(c\hbar\Omega_{\beta 2} / k_B T) - 1}\right),$$

where $\hbar$, $k_B$ and $c$ are the reduced Planck constant, the Boltzmann constant and speed of light, respectively.

## Results and discussion

The vibrational representation of the cubic phase symmetry group in the center of the Brillouin zone is the following:

$$\Gamma_{vib}(Fm3m) = A_{1g}(xx, yy, zz) + E_g(xx, yy, zz) + 2F_{2g}(xz, yz, xy) + F_{1g} + 5F_{1u} + F_{2u}.$$

Given in the brackets are the components of scattering tensor where the corresponding vibrations are active. The site symmetry analysis is carried out on every atom in the primitive unit cell. The preliminary data required are space group and occupied Wyckoff positions [16, 17]. Table 1 and 2 present the symmetry analysis of the cubic and monoclinic phases for two crystals in more details. The vibrational representation of the monoclinic phase

**Table 1.** The symmetry analysis of the elpasolite cubic phase.

| Atom | Wyckoff position | Phonon modes in the center of the Brillouin zone |
|---|---|---|
| Rb | 8c | $F_{2g} + F_{1u}$ |
| K | 4b | $F_{1u}$ |
| Ho, Dy | 4a | $F_{1u}$ |
| F | 24e | $A_{1g} + E_g + F_{2u} + F_{2g} + 2F_{1u} + F_{1g}$ |

Mode classification

| $\Gamma_{Ram} = A_{1g} + E_g + 2F_{2g}$ | $\Gamma_{ir} = 4F_{1u}$ | $\Gamma_{ac} = F_{1u}$ | $\Gamma_{meh} = A_{1g} + E_g + 2F_{2g} + 5F_{1u} + F_{2u} + F_{1g}$ |
|---|---|---|---|

Scattering tensors

| $A_{1g}$ | $E_g$ | $E_g$ | $F_{2g}$ | $F_{2g}$ | $F_{2g}$ |
|---|---|---|---|---|---|
| $\begin{bmatrix} a & 0 & 0 \\ 0 & a & 0 \\ 0 & 0 & a \end{bmatrix}$ | $\begin{bmatrix} b & 0 & 0 \\ 0 & b & 0 \\ 0 & 0 & -2b \end{bmatrix}$ | $\begin{bmatrix} -\sqrt{3b} & 0 & 0 \\ 0 & \sqrt{3b} & 0 \\ 0 & 0 & 0 \end{bmatrix}$ | $\begin{bmatrix} 0 & 0 & 0 \\ 0 & 0 & d \\ 0 & d & 0 \end{bmatrix}$ | $\begin{bmatrix} 0 & 0 & d \\ 0 & 0 & 0 \\ d & 0 & 0 \end{bmatrix}$ | $\begin{bmatrix} 0 & d & 0 \\ d & 0 & 0 \\ 0 & 0 & 0 \end{bmatrix}$ |

**Table 2.** The symmetry analysis of the elpasolite monoclinic phase.

| Atom ($P2_1/n1$) | Wyckoff position | Γ-point phonon modes |
|---|---|---|
| Rb | 4e | $3A_g + 3B_g + 3A_u + 3B_u$ |
| K | 2c | $3A_u + 3B_u$ |
| Ho, Dy | 2a | $3A_u + 3B_u$ |
| $F_1$ | 4e | $3A_g + 3B_g + 3A_u + 3B_u$ |
| $F_2$ | 4e | $3A_g + 3B_g + 3A_u + 3B_u$ |
| $F_3$ | 4e | $3A_g + 3B_g + 3A_u + 3B_u$ |
| | Modes classification | |
| $\Gamma_{Ram} = 12A_g + 12B_g$ | $\Gamma_{ir} = 17A_u + 16B_u$<br>$\Gamma_{ac} = A_u + 2B_u$ | $\Gamma_{meh} = 12A_g + 12B_g + 18A_u + 18B_u$ |
| | Raman tensor | |
| $A_g$ | | $B_g$ |
| $\begin{bmatrix} a & d & 0 \\ d & b & 0 \\ 0 & 0 & c \end{bmatrix}$ | | $\begin{bmatrix} 0 & 0 & e \\ 0 & 0 & f \\ e & f & 0 \end{bmatrix}$ |

symmetry group in the center of the Brillouin zone is the following:

$$\Gamma_{\text{vib}}(P12_1/n1) = 12A_g(xx, yy, zz, xy, yx) + 12B_g(xz, yz, zx, zy) + 18A_u + 18B_u.$$

Table 3 shows assignments and experimental band positions for $Rb_2KScF_6$ and $Rb_2KInF_6$ in the cubic phase. Earlier polarized Raman spectra of isostructural crystals $Rb_2KScF_6$ and $Rb_2NaYF_6$ were studied in [7, 18], and numerical simulations of these spectra for $Rb_2KHoF_6$ and $Rb_2KDyF_6$ performed by both ab initio [7, 19, 20] and empirical [18] approaches helped us to interpret the experimental spectra of $Rb_2KHoF_6$ and $Rb_2KDyF_6$. Experimental band positions and intensities distributions for these crystals are only slightly different from those for $Rb_2KScF_6$ and $Rb_2KInF_6$.

The spectra transformation with temperature is presented in Figure 1a, b. The spectra in the cubic phase (higher temperatures) could be subdivided in three parts, corresponding to vibrations of structural elements: region of lattice vibrations below 150 $cm^{-1}$; F–(Ho, Dy)–F bending region, 150–300 $cm^{-1}$; (Ho, Dy)–F stretching region, 300–600 $cm^{-1}$. Raman spectra of $Rb_2KHoF_6$ crystal are distorted due to the fluorescence processes (Figure 1a). We couldn't analyze in detail the behavior of the $E_g$ symmetry $HoF_6$ stretching mode of $Rb_2KHoF_6$ crystal due to its rather weak intensity.

According to phase diagram in Table 4 one can expect the appearance of new lines at the low temperatures. The phase transition from cubic to monoclinic phase is accompanied with doubling of the primitive cell volume. The modes corresponding to X (0, 0, $\pi$/a) point of the Brillouin zone are Raman inactive in the cubic phase, however, as one can see from the correlation diagram in Table 4, their activation should be observed below the transition point.

The behavior of low wavenumber lines at cooling is presented in Figure 2. New lines appear below phase transition temperature in the both crystals. One can see some anomalies of the behavior of Raman lines with temperature. We observed phase transitions at 380 K for $Rb_2KHoF_6$ and at 392 K for $Rb_2KDyF_6$. We think that all splitting of the lines connected with these phase transitions. The appearance of a new line just below transition points is connected with doubling of the primitive cell that activates one lattice mode of X point of

**Table 3.** Line assignments and positions in the cubic phase.

| Irreducible representation | Eigenvector of normal mode | [this work] $Rb_2KHoF_6$ $cm^{-1}$ | [this work] $Rb_2KDyF_6$ $cm^{-1}$ | [7] $Rb_2KScF_6$ $cm^{-1}$ | [8] $Rb_2KInF_6$ $cm^{-1}$ |
|---|---|---|---|---|---|
| $A_{1g}$ | 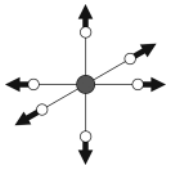 | 472 | 470 | 505 | 507 |
| $E_g$ | 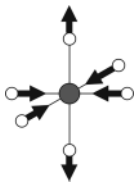 | | 380 | 390 | 379 |
| $F_{2g}$ | 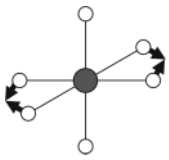 | 204 | 202 | 230 | 218 |
| $F_{2g}$ | | 61 | 65 | 89 | 69 |

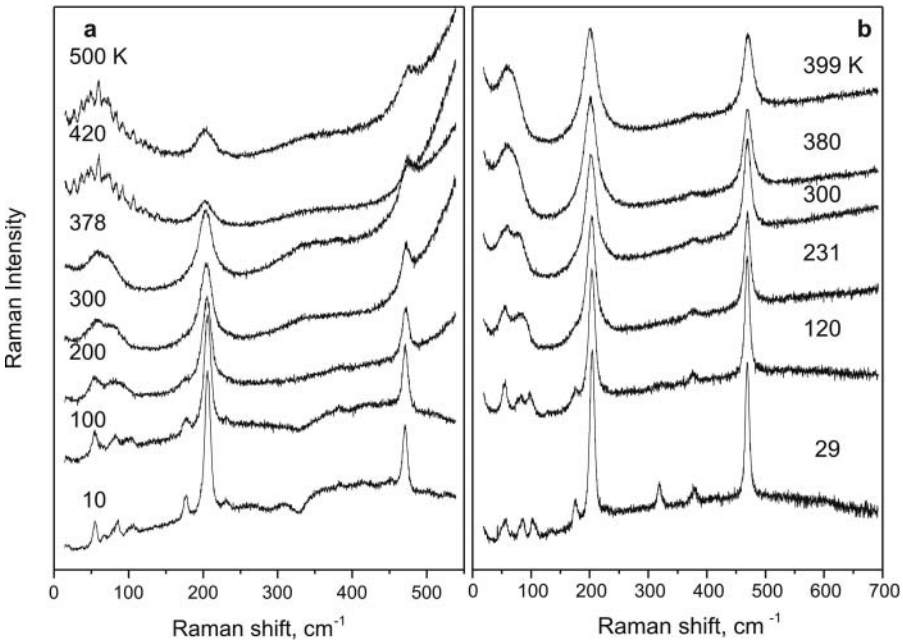


**Figure 1.** Temperature transformation of Raman spectra (a – $Rb_2KHoF_6$, b – $Rb_2KDyF_6$).

**Table 4.** Correlation diagram of the vibrational modes for the cubic and monoclinic symmetries of the elpasolites. Only modes active in Raman spectra of the monoclinic phase are shown.

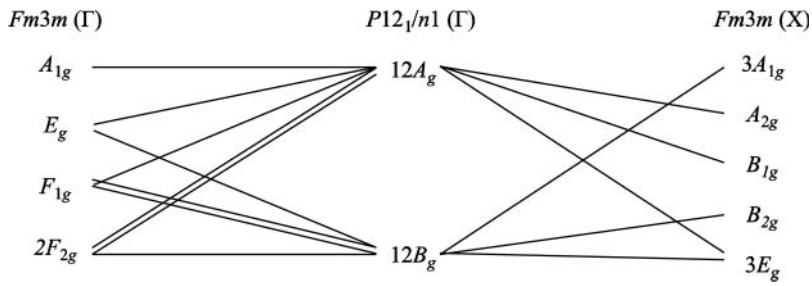


the Brillouin zone. According to correlation diagram (Table 4) we can also wait for splitting of triple degenerated ($F_{2g}$) Raman active lattice mode as well as the same splitting of that new mode, but these splittings seems to be too small to be observed just below transition points. According to the experimental data [21] the monoclinic angle of the unit cell of $Rb_2KHoF_6$ starts to grow gradually only below 250 K, that makes these splittings clearly visible.

The parts of the spectra connected with bending of $Ho(Dy)F_6$ groups change not so significantly. Line position changes from 202 $cm^{-1}$ to 206 $cm^{-1}$ within studied temperature range in $Rb_2KHoF_6$ and from 201 $cm^{-1}$ to 204 $cm^{-1}$ in $Rb_2KDyF_6$ without jumps.

The temperature dependences of the peak position of the internal mode ($A_{1g}$ symmetry) and it's approximation for the both crystals is given in Figure 3. The previous investigations of the temperature phase transitions in $Rb_2KScF_6$, $Rb_2KInF_6$, $Rb_2NaYF_6$ crystals showed that high wavenumber parts of the spectra almost don't change with temperature [7, 8, 18]. But in these experiments one can clearly see the anomalous $\lambda$-shaped spike of the line position at the transition temperature in $Rb_2KHoF_6$. The abrupt changes of the mode positions indicate that the structural transitions in the both crystals are of the first order. As contrasted to the double perovskite crystals with two temperature phase transitions the significant changes in

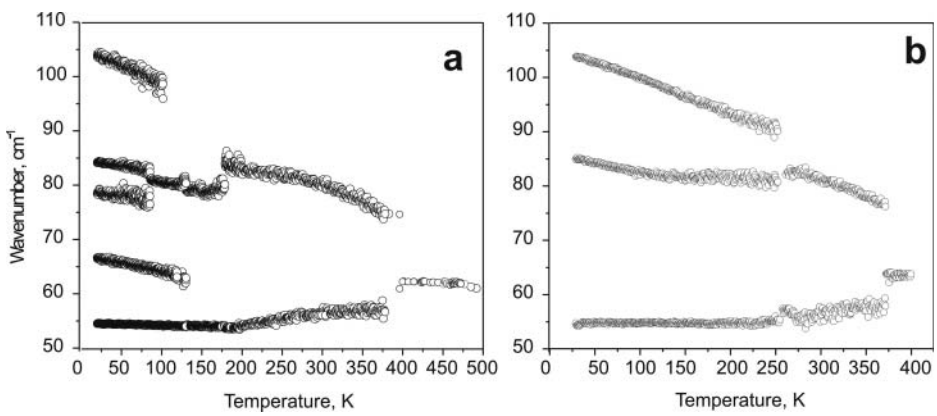


**Figure 2.** Temperature dependences of the low wavenumber modes (a – $Rb_2KHoF_6$, b – $Rb_2KDyF_6$).

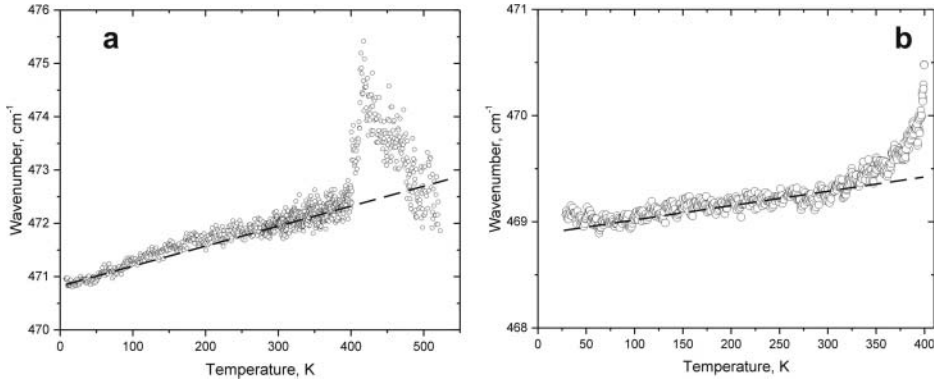


**Figure 3.** Temperature dependence of the full symmetry internal mode position (a – $Rb_2KHoF_6$, b – $Rb_2KDyF_6$). Dashed curves – data approximations.

Raman spectra occur in the (Ho, Dy)–F stretching region. This investigation points to the considerable role of $CX_6$ octahedra rotation in the temperature phase transition.

## Funding

This work was partly supported by Russian Foundation for Basic Research Grant no 16-02-00102, SS-924.2014.2.

## Refrences

1. J. M. Dance, J. Grannec, A. Tressaud, and M. Moreno, ESR Investigation of Phase Transitions in Some Elpasolite-Type Fluorides. *Phys Stat Sol (b).* **173**, 579–586 (1992).
2. M. V. Gorev, K. S. Aleksandrov, A. Tressaud, J. Grannec, and M. Couzi, Phase transitions in elpasolites (ordered perovskites). *Mat Sci Engin R.* **24**, 81–151 (1998).
3. I. N. Flerov, M. V. Gorev, K. S. Aleksandrov, A. Tressaud, and V. D. Fokina, Ferroelastic phase transitions in fluorides with cryolite and elpasolite structures. *Cryst Rep.* **49**, 100–107 (2004).
4. A. M. Woods, R. S. Sinkovits, J. C. Charpie, W. L. Huang, R. H. Bartram, and A. R. Rossi, Computer modeling of the optical properties of substitutional chromium impurities in halide elpasolites. *J Phys Chem Sol.* **54**, 543–552 (1993).
4. A. S. Krylov, S. N. Krylova, A. N. Vtyurin, N. V. Surovtsev, V. N. Voronov, and A. S. Oreshonkov, Raman Spectra and Phase Transitions in $Rb_2KInF_6$ Elpasolite. *Cryst Rep.* **56**, 22–27 (2011).
5. A. N. Vtyurin, A. S. Krylov, S. V. Goryainov, S. N. Krylova, and V. N. Voronov, Raman spectroscopic study of the phase transitions induced by hydrostatic pressure in $Rb_2KScF_6$ crystal. *Phys Solid Stat.* **48**, 1070–1072 (2006).
6. A. S. Krylov, A. Bulou, and S. N. Krylova, Symmetry analysis of calculated vibrational spectra of $Rb_2KScF_6$ crystal. *Comput Mater Sci.* **36**, 221–224 (2006).
7. S. N. Krylova, A. N. Vtyurin, A. Bulou, A. S. Krylov, and N. G. Zamkova, Lattice dynamics and Raman scattering spectrum of elpasolite $Rb_2KScF_6$: comparative analysis. *Phys Sol Stat.* **46**, 1311–1319 (2004).
8. A. S. Krylov, S. N. Krylova, A. N. Vtyurin, V. N. Voronov, and A. S. Oreshonkov, Raman scattering study of temperature phase transitions of $Rb_2KInF_6$ crystal. *Ferroelectrics.* **416**, 95–100 (2011).
9. G. P. Knudsen, Soft mode and structural phase transition in the cubic elpasolite $Cs_2NaNdCl_6$. *Solid Stat Commun.* **49**, 1045–1047 (1984).

10. W. Buhrer, and H. U. Gudel, Soft rotatory mode and structural phase transition in the rare-earth bromo-elpasolites $Cs_2NaReBr_6$. *J Phys C: Solid Stat Phys.* **20**, 3809–3821 (1987).
11. M. Couzi, S. Khaïroun, and A. Tressaud, Structural phase transitions in $Rb_2KM^{III}F_6$ elpasolites. Raman scattering and group-theoretical studies of $Rb_2KFeF_6$ and $Rb_2KYF_6$. *Phys stat sol (a).* **98**, 423–434 (1986).
12. B. Nissen-Sobocińska, W. Strek, J. Hanuza, K. Hermanowicz, G. Denisenko, K. S. Aleksandrov, and V. N. Voronov, Vibronic spectra of $Rb_2NaTmF_6$ elpasolite single crystal. *J Appl Spectr.* **62**, 877–885 (1995).
13. P. A. Tanner, and L. Yu-Long, Electronic Raman, infrared absorption and visible luminescence spectrum of $Cs_2NaEuCl_6$. *J Alloys Comp.* **204**, 93–100 (1994).
14. E. J. Veenendaal, H. B. Brom, and J. Ihringer, Structural phase transition in the cubic elpasolite $Rb_2NaHoF_6$. *Physica B+C.* **114**, 31–36 (1982).
15. M. V. Gorev, I. N. Flerov, V. N. Voronov, and S. V. Misyul', Pressure – temperature phase diagrams of elpasolites $Rb_2KB^{3+}F_6$ ($B^{3+}$ = Ho, Dy, Tb). *Phys Sol Stat.* **35**, 524–527 (1993).
16. D. L. Rousseau, R. P. Bauman, and S. P. Porto, Normal mode determination in crystals. *J Raman Spectr.* **10**, 253–290 (1981).
17. E. Kroumova, M. I. Aroyo, J. M. Perez Mato, A. Kirov, C. Capillas, S. Ivantchev, and H. Wondratschek, Bilbao Crystallographic Server: useful databases and tools for phase transitions studies. *Phase Transit.* **76**, 155–170 (2003).
18. A. S. Krylov, A. N. Vtyurin, A. S. Oreshonkov, V. N. Voronov, and S. N. Krylova, Structural transformations in a single-crystal $Rb_2NaYF_6$: Raman scattering study. *J Raman Spectrosc.* **44**, 763–769 (2013).
19. A. S. Krylov, A. Bulou, S. N. Krylova, V. N. Voronov, A. N. Vtyurin, and N. G. Zamkova, Symmetry analysis of calculated vibrational spectra of $Rb_2KScF_6$ crystal. *Comput Mater Sci.* **36**, 221–224 (2006).
20. V. I. Zinenko, and N. G. Zamkova, Lattice dynamics and statistical mechanics structure phase transition Fm3m – I4/m in $Rb_2KInF_6$ crystal. *Phys Solid Stat.* **43**, 2193–2203 (2001).
21. I. N. Safonov, S. V. Misyul', M. S. Molokeev, and M. P. Ivliev, Structural transformations and phenomenological description of the formation of phase states in elpasolites $Cs_2RbDyF_6$ and $Rb_2KB'F_6$ (B′ = Ho, Dy, Tb). *Phys Solid Stat.* **57**, 491–498 (2015).